



**HAL**  
open science

## Butene Emissions From Coastal Ecosystems May Contribute to New Particle Formation

Chiara Giorio, Jean-François Doussin, Barbara d'Anna, Sébastien Mas,  
Daniele Filippi, Cyrielle Denjean, Marc Daniel Mallet, Thierry Bourrienne,  
Frédéric Burnet, Mathieu Cazaunau, et al.

► **To cite this version:**

Chiara Giorio, Jean-François Doussin, Barbara d'Anna, Sébastien Mas, Daniele Filippi, et al.. Butene Emissions From Coastal Ecosystems May Contribute to New Particle Formation. *Geophysical Research Letters*, 2022, 49, 10.1029/2022GL098770 . insu-03749606

**HAL Id: insu-03749606**

**<https://insu.hal.science/insu-03749606>**

Submitted on 11 Aug 2022

**HAL** is a multi-disciplinary open access archive for the deposit and dissemination of scientific research documents, whether they are published or not. The documents may come from teaching and research institutions in France or abroad, or from public or private research centers.

L'archive ouverte pluridisciplinaire **HAL**, est destinée au dépôt et à la diffusion de documents scientifiques de niveau recherche, publiés ou non, émanant des établissements d'enseignement et de recherche français ou étrangers, des laboratoires publics ou privés.



Distributed under a Creative Commons Attribution 4.0 International License

# Geophysical Research Letters<sup>®</sup>



## RESEARCH LETTER

10.1029/2022GL098770

## Butene Emissions From Coastal Ecosystems May Contribute to New Particle Formation

### Key Points:

- Marine biogenic emissions of reactive volatile organic compounds previously thought to be anthropogenic
- Massive emissions of butenes from the coastal part of the Benguela upwelling system
- Emissions of butenes may contribute to new particle formation in the marine boundary layer

Chiara Giorio<sup>1,2</sup> , Jean-François Doussin<sup>3</sup> , Barbara D'Anna<sup>4</sup> , Sébastien Mas<sup>5</sup>, Daniele Filippi<sup>1,2</sup>, Cyrielle Denjean<sup>6</sup> , Marc Daniel Mallet<sup>3,7</sup> , Thierry Bourriane<sup>6</sup>, Frédéric Burnet<sup>6</sup>, Mathieu Cazaunau<sup>3</sup> , Chibo Chikwillilwa<sup>8</sup>, Karine Desboeufs<sup>3</sup>, Anaïs Feron<sup>3</sup>, Vincent Michoud<sup>3</sup>, Andreas Namwoonde<sup>8</sup> , Meinrat O. Andreae<sup>9,10,11</sup> , Stuart J. Piketh<sup>12</sup>, and Paola Formenti<sup>3</sup> 

<sup>1</sup>Yusuf Hamied Department of Chemistry, University of Cambridge, Cambridge, UK, <sup>2</sup>Dipartimento di Scienze Chimiche, Università degli Studi di Padova, Padova, Italy, <sup>3</sup>Université de Paris Cité and Univ Paris Est Creteil, CNRS, LISA, Paris, France, <sup>4</sup>Aix Marseille University, UMR CNRS 7376, LCE, Marseille, France, <sup>5</sup>Plateforme d'écologie marine expérimentale MEDIMEER, UMS3282 OSU OREME, Université de Montpellier, CNRS/IRD, Sète, France, <sup>6</sup>CNRM, Université de Toulouse, Météo-France, CNRS, Toulouse, France, <sup>7</sup>Australian Antarctic Program Partnership, Institute for Marine and Antarctic Studies, University of Tasmania, Hobart, TAS, Australia, <sup>8</sup>Sam Nujoma Marine and Coastal Resources Research Centre, University of Namibia, Henties Bay, Namibia, <sup>9</sup>Max Planck Institute for Chemistry, Mainz, Germany, <sup>10</sup>Scripps Institution of Oceanography, University of California, San Diego, La Jolla, CA, USA, <sup>11</sup>Department of Geology and Geophysics, King Saud University, Riyadh, Saudi Arabia, <sup>12</sup>Unit for Environmental Science and Management, North-West University, Potchefstroom, North-West, South Africa

### Supporting Information:

Supporting Information may be found in the online version of this article.

### Correspondence to:

C. Giorio,  
chiara.giorio@atm.ch.cam.ac.uk

### Citation:

Giorio, C., Doussin, J.-F., D'Anna, B., Mas, S., Filippi, D., Denjean, C., et al. (2022). Butene emissions from coastal ecosystems may contribute to new particle formation. *Geophysical Research Letters*, 49, e2022GL098770. <https://doi.org/10.1029/2022GL098770>

Received 18 MAR 2022  
Accepted 6 MAY 2022

**Abstract** Marine ecosystems are important drivers of the global climate system. They emit volatile species into the atmosphere, involved in complex reaction cycles that influence the lifetime of greenhouse gases. Sea spray and marine biogenic aerosols affect Earth's climate by scattering solar radiation and controlling cloud microphysical properties. Here we show larger than expected marine biogenic emissions of butenes, three orders of magnitude higher than dimethyl sulfide, produced by the coastal part of the Benguela upwelling system, one of the most productive marine ecosystems in the world. We show that these emissions may contribute to new particle formation in the atmosphere within the marine boundary layer through production of Criegee intermediates that oxidize SO<sub>2</sub> to H<sub>2</sub>SO<sub>4</sub>. Butene emissions from the marine biota may affect air quality and climate through ozone, secondary organic aerosol, and cloud condensation nuclei formation even in pristine regions of the world. Our results indicate a potentially important role of butene emissions in marine particle formation that requires investigation in other regions.

**Plain Language Summary** Marine biogenic emissions of volatile organic compounds (VOCs) are key drivers of the Earth's climatic system, but they are not considered in climate models, except for dimethyl sulfide (DMS). We observed massive concentrations of reactive VOCs, especially butenes, in ambient air at a pristine coastal site on the west coast of the southern African continent. These strong emissions originated from the coastal part of the Benguela ecosystem and may have contributed to new particle formation in the marine boundary layer. According to our observations, butenes can be found at concentrations orders of magnitude larger than DMS in highly productive coastal environments and thus their climatic impact requires investigation.

## 1. Introduction

Marine ecosystems, which are a network of interactions among different organisms, are an important source of volatile organic compounds (VOCs) and organic-rich primary and secondary aerosols (Brooks & Thornton, 2018; Mayer et al., 2020; O'Dowd et al., 2015; Schneider et al., 2019; Trueblood et al., 2019; Vaattovaara et al., 2006). Coastal environments, where unique and often highly productive ecosystems develop and gas transfer across the air-sea interface is enhanced (e.g., by evaporation and bubble-bursting), may be strong emitters of VOCs, as already demonstrated by their dominance for methane oceanic emission (Weber et al., 2019). Decomposition of microalgae is a known source of sulfur-containing compounds in the air such as dihydrogen sulfide, dimethyl sulfide (DMS), dimethyl disulfide (DMDS), dimethyl trisulfide, methanethiol, isopropyl thiol, diisopropyl disulfide, and diisopropyl trisulfide (Achyuthan et al., 2017). Various phytoplankton species are also isoprene emitters with observed isoprene mixing ratios in oceanic and coastal sites across the globe as high as 300 ppt in

© 2022. The Authors.

This is an open access article under the terms of the [Creative Commons Attribution License](https://creativecommons.org/licenses/by/4.0/), which permits use, distribution and reproduction in any medium, provided the original work is properly cited.

the absence of terrestrial sources (Shaw et al., 2010). Marine terpenoids are produced by micro- and macroalgae, sponges, and corals, as well as cyanobacteria (Achyuthan et al., 2017; Shaw et al., 2010). The VOC emissions from marine phytoplankton also include halogenated compounds, such as methyl chloride, methyl bromide, methyl iodide, as well as iodine (Achyuthan et al., 2017), but also chlorobenzene and p-dichlorobenzene which are typically considered anthropogenic compounds (Colomb et al., 2008). Besides the aforementioned compounds, many other classes of VOCs are produced by microalgae such as alcohols, esters, aldehydes, hydrocarbons (both aliphatic and aromatic), terpenes and terpene derivatives, ketones, furans, carboxylic acids, fatty acids, and carotenoid derivatives (Achyuthan et al., 2017; Ali, 2004; Jerković et al., 2018). Bacteria are also VOC emitters; cyanobacteria contribute to alkane production, predominantly C15 and C17 alkanes (Lea-Smith et al., 2015). A study on Antarctic bacteria showed production of a wide range of volatiles such as S-containing compounds, 2-butene, 1,3-butadiene, furan, acetone, and other ketones, alcohols, and esters (Papaleo et al., 2013).

Emitted VOCs can undergo oxidation in the atmosphere leading to the formation of secondary organic aerosol (SOA), which may grow to be active as cloud condensation nuclei (CCNs) thus affecting the Earth's climate (Zheng et al., 2021). A notable example is DMS, a marine biogenic marker that is an efficient aerosol and cloud droplet producer (Grandey & Wang, 2015). According to the CLAW hypothesis, DMS emissions are key in the establishment of a feedback loop between global warming, enhanced production of marine plankton, and increased emissions of DMS leading to CCN production. As the reflectance of clouds is sensitive to CCN concentrations, biogenic emissions would lead to cooling and therefore stabilization of atmospheric temperature (Charlson et al., 1987). Strong support for the CLAW hypothesis came from observation of DMS and aerosol production in the tropical South Atlantic (Andreae et al., 1995), although there is still a debate on whether the feedback loop would lead to overall cooling or warming of the atmosphere. More recent studies questioned the validity of the CLAW hypothesis and pointed out that sources of CCNs and cloud response to them are much more complex than previously anticipated (Quinn and Bates, 2011) and that chemical composition of particles with 100–200 nm diameter controls CCN in the marine boundary layer (Saliba et al., 2020). Reactive VOCs can also impact the atmospheric ozone budget as they are implicated in complex reaction cycles that can either deplete or produce tropospheric ozone (Derwent, 2007).

The Benguela upwelling system, off the west coast of southern Africa, is a well-known ecosystem in which upwelling pulses of nutrient-rich waters induce high biological production (Ohde & Dadou, 2018). As a consequence of upwelling along the north coast of Namibia, phytoplankton blooms are frequent, although highly variable in both biomass and species composition (Lamont et al., 2019).

To assess the strength and diversity of VOC sources in highly productive coastal environments and their ability to contribute to new particle formation, we made continuous measurements of VOCs and aerosol size distributions during the August–September 2017 Aerosols, Radiation and Clouds in southern Africa (AEROCLO-SA) field campaign at the Sam Nujoma Marine and Coastal Resources Research Centre (SANUMARC) of the University of Namibia at Henties Bay (22°6'S, 14°30'E; 20 m above mean sea level) (Formenti et al., 2019). SANUMARC is located right above the beach at about 100 m from the ocean (on the west) (Text S1 in Supporting Information S1).

## 2. Materials and Methods

### 2.1. VOC Measurements

Volatile organic compound (VOC) measurements were conducted between 23 August and 12 September 2017. The instrumentation deployed was part of the Portable Gas and aerosol Sampling Units (PEGASUS) mobile platform (Formenti et al., 2019). VOC measurements were performed using a KORE Inc™ (second generation) high-resolution Proton Transfer Reaction Time-of-Flight Mass Spectrometer (PTR-ToF-MS). Ambient air was sampled through a 1.5-m long Silcosteel® coated stainless steel tube (2.1 mm inner diameter), at a constant flow rate of about 5 cm<sup>3</sup> s<sup>-1</sup> (estimated residence time below 2 s) as used in previous studies (Duncan et al., 2017). Pressure in the glow discharge region was set to 2.00 hPa while pressure in the proton transfer reaction tube was set to 1.33 hPa, temperature to 60°C and voltage to 390 V, leading to an E/N of 142 Td (1 Td = 10<sup>-17</sup> V cm<sup>2</sup>). These settings were optimized before the start of the campaign and checked throughout the campaign using standard VOC mixtures diluted with an Ionicon Analytik gas calibration unit (GCU) at 70% relative humidity and 25°C. Three different standard VOC mixtures (containing among others trans-but-2-ene, but-1-ene, and

cis-but-2-ene) were used for optimisation and calibration of the instrumental signals (Text S2 in Supporting Information S1).

During the campaign, spectra were integrated over 5 min and blank measurements were done at ambient relative humidity three times per day using the catalytic converter of the GCU to subtract potential contaminations from the sampling lines.

Data analysis was done using GRAMS/AI version 9.3. VOC concentrations were obtained by external calibration for compounds for which gas standards were available or estimated based on the rate constant of the proton-transfer reaction from  $\text{H}_3\text{O}^+$  only, or from both  $\text{H}_3\text{O}^+$  and  $(\text{H}_2\text{O})\text{H}_3\text{O}^+$  (Ellis & Mayhew, 2014), depending on the proton affinity of the compound, whenever identification was possible. Ion transmission versus  $m/z$  was evaluated using the GCU and NPL gas standards. Details of methods used for quantification for each peak and reaction rate constants used can be found in the AEROCLO-sA database ([https://baobab.sedoo.fr/Data-Search/?-datsId=1773&project\\_name=AEROCLO](https://baobab.sedoo.fr/Data-Search/?-datsId=1773&project_name=AEROCLO), Accessed 9 November 2021).

## 2.2. Analysis of Ocean Foam and Ocean Water

Reference spectra of ocean water and ocean foam collected on the beach next to the sampling station were also obtained. The formation of ocean foam was frequently observed during the campaign. Samples of foam and water were collected during particularly intense episodes on 9 September at noon and in the morning of 10 September. The foam sample collected on 9 of September was left to dry at room temperature ( $\sim 12^\circ\text{C}$ ) overnight. Foam samples collected on 10 September were kept wet, and water samples, collected on the same day, were filtered. All samples were kept in the fridge in the dark at  $4^\circ\text{C}$  until analysis. Reference spectra were recorded on the 12 September in the headspace of a 50 mL falcon tube containing 10 mL of sample on the bottom. Measurements of the head-space samples were done at a constant flow rate of  $150\text{ mL min}^{-1}$  using zero air as back-up flow to keep constant pressure in the falcon tube. PTR-ToF-MS settings were the same used for ambient measurements.

For flow cytometric analyses, samples of 10 mL foam and seawater for microbial plankton ( $<20\ \mu\text{m}$ ) analyses were fixed with formal (4% final concentration) and then stored at  $-20^\circ\text{C}$  until analysis. The samples were analyzed with FacsCanto II cytometer (3-laser, 8-color (4-2-2), BD Biosciences) equipped with a 20 mW 488 nm coherent sapphire solid state blue laser. It permits the evaluation of the abundance of phytoplankton (cyanobacteria, pico ( $<2\ \mu\text{m}$ ) and nanophytoplankton ( $2\text{--}20\ \mu\text{m}$ )) (Pecqueur et al., 2011), heterotrophic bacteria (Lebaron et al., 2001) and viruses (Brussaard, 2004). The cyanobacteria population (*Synechococcus*) was discriminated from other phytoplanktons by its orange fluorescence (due to the presence of phycoerythrin) on the orange versus red fluorescence cytogram (Waterbury et al., 1979).

## 2.3. Satellite Retrieved Chlorophyll-a Concentrations

Average chlorophyll-a (Chl-a) concentrations were retrieved from the “Ocean color daily data from 1997 to present derived from satellite observations” product from the Copernicus Climate Data Store (CDS, 2021).

## 2.4. Aerosol Size Distributions

Ambient aerosol number size distribution data from 10 nm to  $30\ \mu\text{m}$  were obtained by a combination of standard optical and electrical mobility analyzers. The aerosol number size distribution from 10.9 to 461.4 nm in diameter was measured by a Scanning Mobility Particle Sizer (SMPS), comprising of a Differential Mobility Analyzer (DMA, model 3,080, TSI Inc., Shoreview, MN) and a Condensation Particle Counter (CPC, model 3,772, TSI Inc., Shoreview, MN) operated at  $1.0/5.0\ \text{L min}^{-1}$  aerosol/sheath flow rate on a 3-min averaging time, including 2.5 min of sampling of the size distribution data (scan up period) and 30 s scan retrace time period. The SMPS operated from a certified Total Suspended Particulate (TSP) sampling head (Rupprecht and Patashnick, Albany, NY, USA), followed by a cyclone impactor cutting off aerosol particles larger than  $1\ \mu\text{m}$  in aerodynamic diameter (using a flow rate of  $16\ \text{L min}^{-1}$ ). The ambient aerosol number size distribution from 0.25 to  $32\ \mu\text{m}$  in diameter was measured on 32 size classes by an Optical Particle Counter (OPC, model 1.109, Grimm Aerosol Technik, Ainring, Germany) operated at  $1.2\ \text{L min}^{-1}$  aerosol flow rate on a 6-s averaging time. The GRIMM OPC sampled from a high-volume wind-orientable sampling inlet developed at LISA for the African Monsoon Multidisciplinary

Analysis project (Rajot et al., 2008). Neither the SMPS nor the GRIMM OPC inlets were connected to a drier, therefore the size distributions reported are for ambient conditions (RH approximately 40% in the inlet).

The combination of the number size distributions measured by the SMPS and the GRIMM OPC to yield the full aerosol number size distribution required some corrective steps. Because of their operating principles, neither the SMPS nor the GRIMM OPC express the number size distribution as a function of the particle geometric diameter, which needs to be estimated based on the properties of the ambient aerosols. For the SMPS, the conversion of the operating electrical mobility diameter ( $D_m$ ) to the equivalent sphere geometric diameter ( $D_g$ ) depends on particle dry dynamic shape factor ( $\chi$ ), which is equal to 1 for spherical particles and larger than unity for non-spherical aerosols (DeCarlo et al., 2004). For the GRIMM OPC, the conversion of the optical equivalent diameter ( $D_o$ ) to  $D_g$  is based on the knowledge of the complex refractive index ( $m$ ) of the ambient aerosols (Hinds, 1999; Wendisch & Brenguier, 2013).

Additionally, both measured size distributions need to be corrected for the size-dependent losses of particles that occur during sampling at the inlet and transport through the sampling lines due to various processes (e.g., diffusion, sedimentation, inertial deposition), in non-isokinetic conditions and a bent tubing. These corrections were implemented using the Particle Loss Calculator program developed by Von Der Weiden et al. (2009). Based on the measured dimensions of the sampling lines, the campaign-average wind speed of  $6 \text{ L min}^{-1}$ , and the equivalent sphere aerodynamic diameter ( $D_a$ ) estimated from  $D_g$  as  $D_a = D_g \sqrt{\rho_p / \rho_0}$ , where  $\rho_p$  is the ambient particle mass density and  $\rho_0$  is the unit reference particle mass density.

Finally, in order to merge the measured SMPS and GRIMM OPC size distributions, an iterative approach was implemented. The physical aerosol parameters ( $\chi$ ,  $m$ ,  $\rho$ ) were varied until the size-dependent loss corrected SMPS and GRIMM OPC size distributions agreed on their nominal overlap region (0.25–0.46 nm). The best agreement was obtained with the following average values:  $\chi = 1$  and  $m = 1.6 - 0.002i$  at 655 nm. The best agreement between the evaluated size distribution and measured mass concentrations (not shown) was achieved by adjusting the particle effective density ( $\rho_p$ ) to  $2.7 \text{ g cm}^{-3}$ .

## 2.5. Aerosol Composition

Online aerosol composition was measured using a compact-Time-of-Flight Aerosol Mass Spectrometer (c-ToF-AMS), providing a comprehensive chemical composition of non-refractory  $\text{PM}_{1.0}$ . Data used here were analyzed using the Igor Pro package, Squirrel (version 1.63G), and cumulative peak fitting analysis according to the method described in Müller et al. (2011). Calibration was performed on-site before and after the campaign using ammonium nitrate, ammonium sulfate, sodium chloride, and polystyrene latex spheres. Size-dependent aerodynamic lens transmission efficiency was 30% at 60 nm, 60% at 70 nm, 100% between 80 and 550 nm, 60% at 600 nm, 50% at 700 nm, and 30% at 900 nm (Liu et al., 2007). Analysis of the composition of nebulized ocean water was used to calculate the sea-salt sulfate ( $\text{ss-SO}_4^{2-}$ ) and non-sea-salt sulfate ( $\text{nss-SO}_4^{2-}$ ) fractions based on the measured sulfate-to-chloride ratio.

## 2.6. Calculation of the Condensational Sink, Condensational Growth Rate, and Nucleation Rate

The Condensational Sink (CS, unit  $\text{s}^{-1}$ ), measuring the rate constant for condensation of a gas phase species on pre-existing aerosols, was calculated according to Dal Maso et al. (2002), based on the measured size distribution obtained as described in paragraph “2.4 Aerosol Size Distributions.”

Condensational growth rate and nucleation rate were calculated from SMPS measurements by using the PARGAN (PARTicle Growth And Nucleation) routine in Igor 6.2 (Verheggen & Mozurkewich, 2006). This procedure uses inverse non-linear regression analysis of the general dynamic equation, which describes the evolution of the aerosol size distribution in time due to nucleation, coagulation and condensational growth rates based on consecutive measurements of the aerosol size distribution. The growth rates are obtained by the inverse analysis of the measured change in the aerosol size distribution over time and the nucleation rate is obtained by integrating the particle losses from the time of measurement to the time of nucleation assuming that the diameter of the critical cluster is 1 nm (Verheggen & Mozurkewich, 2006).

All calculations were based on the volatility of sulfuric acid. Although not directly measured, sulfuric acid has been chosen for the calculations because its presence in the particle phase is more than likely (the mass

concentration of sulfate is significant), and because it is known to both promote NPF and contribute to particle growth. Organic compounds also contribute to particle growth, but their identity is not known at the molecular level.

### 2.7. Calculation of the Atmospheric Concentrations of Sulfuric Acid

Atmospheric concentrations of sulfuric acid were estimated using Equation 1 which was adapted from the proxy developed by Yang et al. (2021) and Mikkonen et al. (2011) and takes into account oxidation of SO<sub>2</sub> by both OH radical and stabilized Criegee intermediates (SCIs) produced from the ozonolysis of butenes:

$$[\text{H}_2\text{SO}_4] = \frac{k_1 \cdot [\text{butenes}] \cdot [\text{O}_3] \cdot [\text{SO}_2]}{\text{CS}} + \frac{B \cdot k_2 \cdot \text{Irradiance} \cdot [\text{SO}_2]}{\text{CS} \cdot \text{RH}} \quad (1)$$

where all species concentrations are in molecules/cm<sup>3</sup>, Irradiance is the total irradiance in W/m<sup>2</sup>, CS is the condensational sink in s<sup>-1</sup>, *B* is a scaling factor (2.99 10<sup>5</sup>, calculated by Mikkonen et al. (2011) for Atlanta (US), in high RH conditions), *k*<sub>1</sub> (2.49 10<sup>-30</sup> cm<sup>6</sup>/s) is the rate constant for the oxidation of SO<sub>2</sub> by SCIs (from Equation 9 of Yang et al. (2021)), and *k*<sub>2</sub> is the rate constant for OH oxidation of SO<sub>2</sub> calculated using the formula reported in Mikkonen et al. (2011).

### 2.8. Statistical Analysis

Hierarchical cluster analysis, to compare ambient mass spectra during VOCs peak events with reference mass spectra of ocean foam and water (raw spectra, PTR-ToF-MS), were done using the Euclidean distance (based on peak intensities in counts-per-second), single linkage method in Statsoft Statistica 8.0.

All correlations were done based on *r*-Pearson using Microsoft Excel 2016. Lagged correlations were done using the “ccf” function in the “tseries” package in R studio (R version 3.4.1). For statistical significance we used a 95% confidence level. Correlation strength was defined using the guidelines of Cohen (1988). Unless otherwise stated, correlations were done on data covering the entire campaign.

## 3. Results and Discussion

Our observations (Figure 1) showed the dominance of butenes (C<sub>4</sub>H<sub>9</sub><sup>+</sup> signal, representing the sum of 1-butene, 2-methylpropene, cis-2-butene, and trans-2-butene), which were the most abundant among the VOCs measured (median mixing ratio of 22 ppb, interquartile range of 32 ppb, and maximum of 548 ppb). While the C<sub>4</sub>H<sub>9</sub><sup>+</sup> signal could be also produced from the fragmentation of longer chain compounds, in this case, such a contribution would be minor given that the C<sub>4</sub>H<sub>9</sub><sup>+</sup> signal is orders of magnitude higher than any other longer chain compound. The observed concentrations were substantially higher than those previously observed in marine environments. Very low mixing ratios, below 0.1 ppb, were observed on two cruises in the Mediterranean and Red Seas (Bonsang & Lambert, 1985). Mixing ratios in the ppt range were observed in the Central Pacific, Oki Island of Japan, and at the Mace Head observatory in the North Atlantic (Bourtsoukidis et al., 2019; Donahue & Prinn, 1993; Lewis et al., 2005; Sharma et al., 2000). It is worth noting that none of these studies performed measurements in marine areas characterized by high biological activity. In the Arabian Sea, which on the other hand is biologically productive, average concentrations of 1-butene were in the order of 0.88–1.4 ppb (Tripathi et al., 2020), far lower than the level reported in our study but higher compared to other marine areas.

Marine microorganisms are a known source of butene species. These include marine phytoplankton, notably marine diatoms and nanophytoplanktons (Coccolithophores and Phaeocystis sp.) (Ratte et al., 1995). Bacteria are also butene species emitters (Misztal et al., 2018), although studies in the marine environment have not yet been done. In our study, high concentrations of butenes were associated with winds blowing from the north northwest (NNW) direction (Figure 1), consistent with marine emissions and increased bubble-bursting along the coast. A diverse range of reactive hydrocarbons, mainly mono- and di-unsaturated, were observed, including VOCs previously thought to be markers of anthropogenic emissions such as toluene (Text S2 in Supporting Information S1). Rocco et al. (2021) already observed benzenoids in remote oceanic regions. Other abundant VOCs observed during the campaign were isoprene (C<sub>5</sub>H<sub>9</sub><sup>+</sup>), with median mixing ratios of 70 ppt, methanol (CH<sub>3</sub>O<sup>+</sup>), the most abundant oxygenated VOC with a median mixing ratio of 1.6 ppb, followed by formic acid (CH<sub>3</sub>O<sub>2</sub><sup>+</sup>),

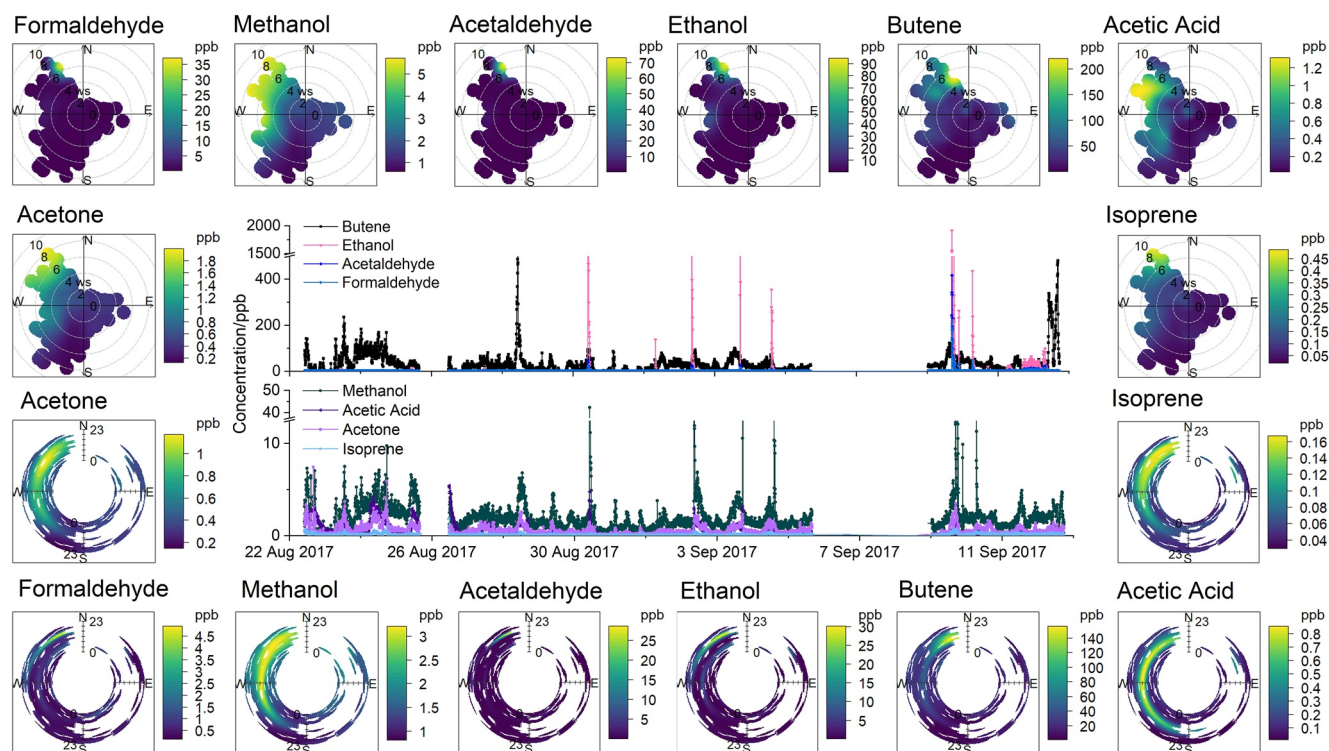


**Figure 1.** Time series, polar plots (wind rose depicting the trend in concentration with wind speed and direction), and polar annulus (wind rose depicting the diurnal trend in concentration with wind direction) of the major volatile organic compounds observed during the Aerosols, Radiation and Clouds in southern Africa field campaign in Henties Bay (Namibia) from 22 August to 12 September 2017.

acetone ( $C_3H_7O^+$ ), formaldehyde ( $CH_3O^+$ ), acetaldehyde ( $C_2H_5O^+$ ), ethanol ( $C_2H_7O^+$ ) and acetic acid ( $C_2H_5O_2^+$ ) with median mixing ratios of 1.0 ppb, 470, 420, 290, 250, and 200 ppt, respectively (Figure 1). For all of these VOCs, higher concentrations were observed when the wind blew from the NW (methanol, acetone, and acetic acid) and NNW (formaldehyde, acetaldehyde, ethanol, butene, and isoprene) directions, consistent with transport of emissions from the Benguela upwelling system. While terrestrial sources of isoprene were dominant in other coastal areas (Arnold et al., 2009; Gantt et al., 2019), the sampling site of this study is surrounded by desert on three sides, and it is far away from any significant terrestrial biogenic source.

During the AEROCLO-sA campaign, we observed the frequent formation of ocean foam along the shoreline (Figure 2a), a typical manifestation of intense biological production (Schilling & Zessner, 2011), which is also evident from the satellite chlorophyll data (Figure 2c). Foam formation is usually linked to a richness of dissolved organic materials (e.g., biogenic lipids, amino acids, carbohydrates, and proteins) released and accumulated at the sea surface. Such organic materials can be produced from the exudation, viral lysis, or decomposition of phytoplankton as well as from broken phytoplankton cells, particularly when whipped up by wind and waves on the coast (Schilling & Zessner, 2011). In addition, foams are remarkably rich and diverse in microorganisms, including bacteria, protists, and algae (Rahlff et al., 2020; Roveillo et al., 2020). During some of the most intense events, samples of ocean foam and water were collected along the coast adjacent to our measurement site. The flow cytometric analyses of marine microorganisms indicated that the ocean foam contained mostly viruses and bacteria, whereas, in the waters, *Synechococcus*, pico- and nanophytoplankton, as well as viruses and bacteria, were detected. Viruses were more than an order of magnitude higher in the foam than in the water (Table 1).

The planktonic microorganisms (heterotrophic bacteria, *synechococcus*, pico- and nanophytoplankton) observed in our ocean water samples have been associated with emission of some VOCs (Lea-Smith et al., 2015; Lin et al., 2013; McKay et al., 1996) and foam formation (Blauw et al., 2010; Hansen et al., 2014). The presence of higher virus concentrations in foam in comparison to ocean water suggests a viral infection of a phytoplankton bloom. The viruses, as well as dissolved organic matter, are released from viral lysis of phytoplanktonic

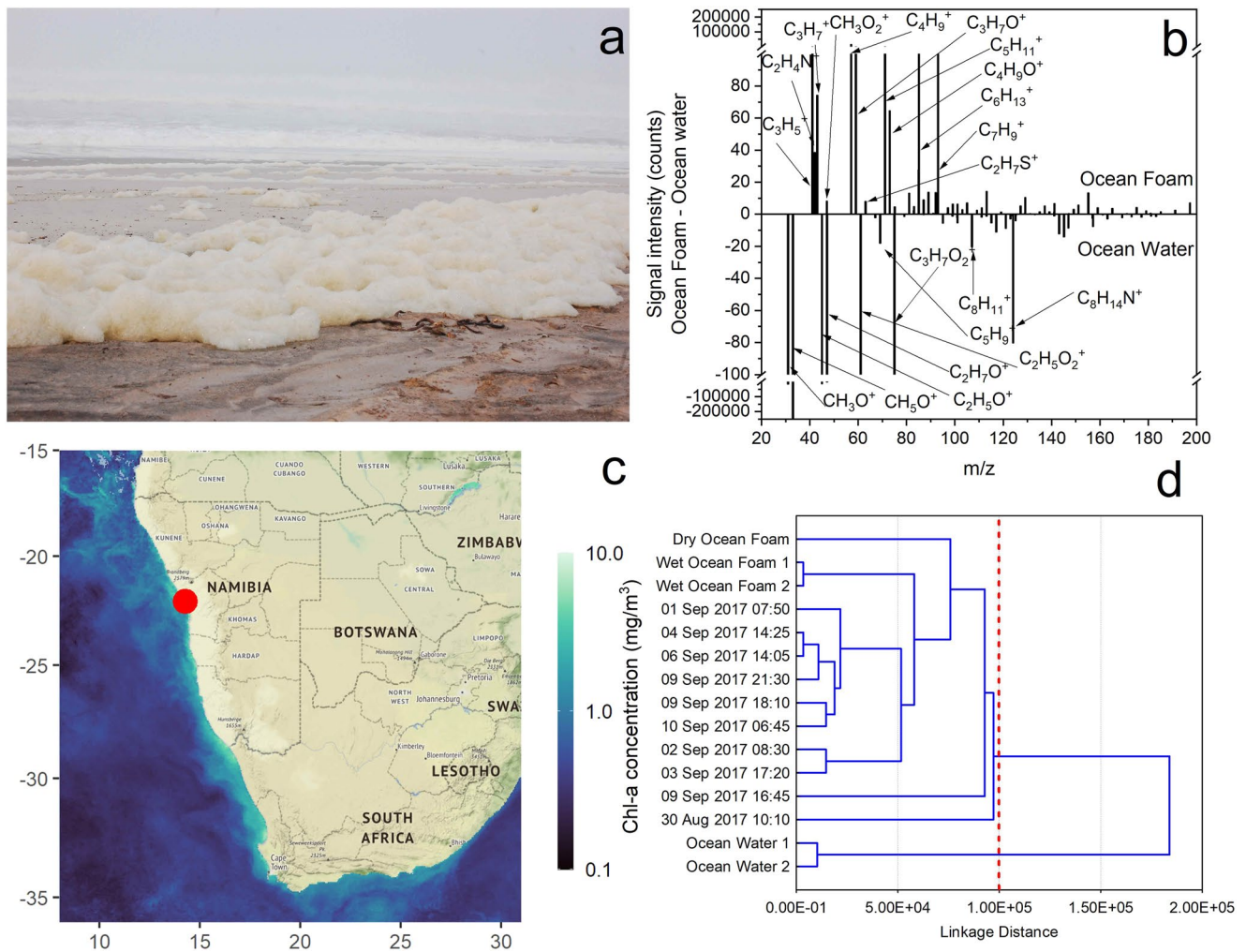


**Figure 2.** Picture of ocean foam forming along the coastline in Henties Bay (Namibia) during the Aerosols, Radiation and Clouds in southern Africa campaign (a), plot depicting the difference in headspace-MS spectra of the ocean foam and filtered ocean water (b), Average chlorophyll-a (Chl-a) concentration for August and September 2017 from MODIS Aqua, VIIRS and OLCI with x-axis in °E and y-axis in °S (c), dendrogram showing the results of the hierarchical cluster analysis (single linkage, Euclidean distance) applied to the mass spectra of the peak events and headspace-MS reference spectra (d). The red dot in panel “c” indicates the sampling site. The vertical red dashed line in panel “d” indicates that samples clustered into two different groups in which ambient samples cluster together with the headspace-MS reference spectra of the ocean foam while headspace-MS reference spectra of ocean water cluster in a separate group. Time is in UTC.

**Table 1**

*Results of the Flow Cytometric Analysis of Ocean Water and Ocean Foam Samples Collected During the Aerosols, Radiation and Clouds in Southern Africa Campaign in Henties Bay*

	Viruses (cells/ mL)	Bacteria (cells/ mL)	Phytoplankton <20 μm (cells/mL)		
			Synechococcus	Picophytoplankton	Nanophytoplankton
Ocean water (09Sep2017)	$6.70 \times 10^7$	$2.95 \times 10^6$	$4.57 \times 10^3$	$1.26 \times 10^3$	$5.79 \times 10^2$
Ocean foam (09Sep2017)	$9.58 \times 10^8$	$1.90 \times 10^6$	nd <sup>a</sup>	nd	nd
Ocean water (10Sep2017)	$6.76 \times 10^7$	$2.50 \times 10^6$	$8.68 \times 10^3$	$2.47 \times 10^3$	$2.20 \times 10^3$
Ocean foam (10Sep2017)	$2.19 \times 10^9$	$3.19 \times 10^6$	nd	nd	nd

<sup>a</sup>nd = not detected.

cells, bloom senescence phase or broken phytoplankton cells, and are accumulated in induced foam (Roveillo et al., 2020; Schilling & Zessner, 2011).

Headspace analysis of the ocean foam and water showed the presence of a wide range of VOCs such as methanol, ethanol, formaldehyde, acetaldehyde, formic acid, acetic acid, butenes, DMS, acetone, methyl ethyl ketone (MEK), and isoprene (Figure 2b). Besides DMS, monoterpenes and isoprene have also been reported to be important in marine environments (Shaw et al., 2010). While monoterpenes were not observed at high concentrations in our head-space samples or throughout the campaign, isoprene was consistently present (Figure 1) and may be emitted by marine plankton in addition to DMS (Achyuthan et al., 2017; Shaw et al., 2010). It is not surprising that isoprene emissions dominated over monoterpene emissions as this was also observed in laboratory studies on phytoplankton monocultures reviewed by Shaw et al. (2010). Previously, many other VOCs have been reported in emissions by the marine biome. Among them, acetaldehyde, methanol, and acetone (as well as isoprene) are important VOCs in the ocean, thought to be conduits for carbon transfer from phytoplankton to bacterioplankton (Halsey et al., 2017). MEK was previously observed in seawater over the Great Barrier Reef (Swan et al., 2016). Laboratory studies on VOC emissions from natural phytoplankton collected at a coastal location in south-eastern North Carolina (US) and algal cultures (marine diatom and dinoflagellate) showed that formaldehyde is both generated and consumed by phytoplankton with variations dependent upon the growth cycle (Nuccio et al., 1995).

The ocean foam spectra are broadly overlapping (in terms of relative intensity of the different VOCs) with the spectra recorded during the VOC peak events (sharp increase in concentration of various VOCs up to the ppm range) observed during the campaign (Figure 1), and the results of the cluster analysis in Figure 2d show that the spectra of ocean foam are more similar to the spectra recorded during the VOCs peak events compared to the spectra of the ocean water. These results suggest that ocean foam may be the main source responsible for the observed VOCs peak events. This, together with the biological analysis of foam and ocean water samples, indicates that the VOC peak events observed during the campaign may be linked to emissions from degradation/breakdown of marine microorganisms (Halsey et al., 2017) and virus-induced phytoplankton cell lysis (Danovaro et al., 2011; Korpi et al., 2009). We have also shown that other VOCs, in addition to the most studied DMS (Halsey et al., 2017), can be produced on a massive scale by coastal ecosystems. Additional information on the source apportionment of observed VOCs can be found in “Text S3 in Supporting Information S1.” While some of these VOCs, such as butenes, were previously considered to be anthropogenic, Henties Bay is not affected by significant anthropogenic sources. Ship traffic is at least 50 km away from Henties Bay and the closest port (Walvis Bay) is more than 100 km away (Tournadre 2014). The area offshore Henties Bay is currently investigated by sea exploration and drilling, however, at the time of the campaign these activities had not yet started ([http://eia.met.gov.na/screening/80\\_galp\\_pel82\\_final\\_eia\\_report\\_final\\_dec\\_2019\\_full\\_report\\_small.pdf](http://eia.met.gov.na/screening/80_galp_pel82_final_eia_report_final_dec_2019_full_report_small.pdf), accessed 5 November 2021). Further, the Omaruru River does not transport pollution from upstream down to Henties Bay. The Omaruru River delta aquifer, approximately 100 km inland (east) of Henties Bay, receives less than 50 mm/year of precipitation, and acts as a barrier for the river which does not flow at Henties Bay (Geyh and Plothner, 1995). A recent study from Rocco et al. (2021) also reported that some VOCs previously thought to be anthropogenic, that is, benzenoids, can be instead emitted by oceanic phytoplankton.

In conjunction with the strong emissions of reactive VOCs, we observed seven new particle formation (NPF) events at the ground-based site during the AEROCLO-sA campaign, on 23 August at around 18h00, 25 August at around 13h00, 31 August at around 14h00, 6 September at around 13h00, 7 September at around 17h00, 8 September at around 15h00, and 9 September at around 15h00. The latter event is shown in Figure 3. All times are reported in West Africa Time (WAT) corresponding to UTC+1.

As shown in Figure 3, some NPF events happened alongside condensation onto pre-existing particles and increase in number concentration of larger particles as opposed to extremely clean conditions. Clean conditions, where condensation onto existing particles would be limited, as observed and modeled in previous studies in the tropical marine boundary layer (Clarke et al., 1998; Pirjola et al., 2000; Russell et al., 1994) and around the Antarctic peninsula (Brean et al., 2021), would be the best conditions for NPF events to occur but strong emissions may lead to NPF even in non-pristine environments, such as megacities in China (Kulmala et al., 2017, 2021).

All events occurred during daylight hours ranging from midday to early/late afternoon, and were, therefore, likely to be driven by a combination of marine biogenic emissions and photochemistry. The diurnal trends of the gas-phase compounds (Figure 3) show that these NPF events were preceded by an increase in biogenic

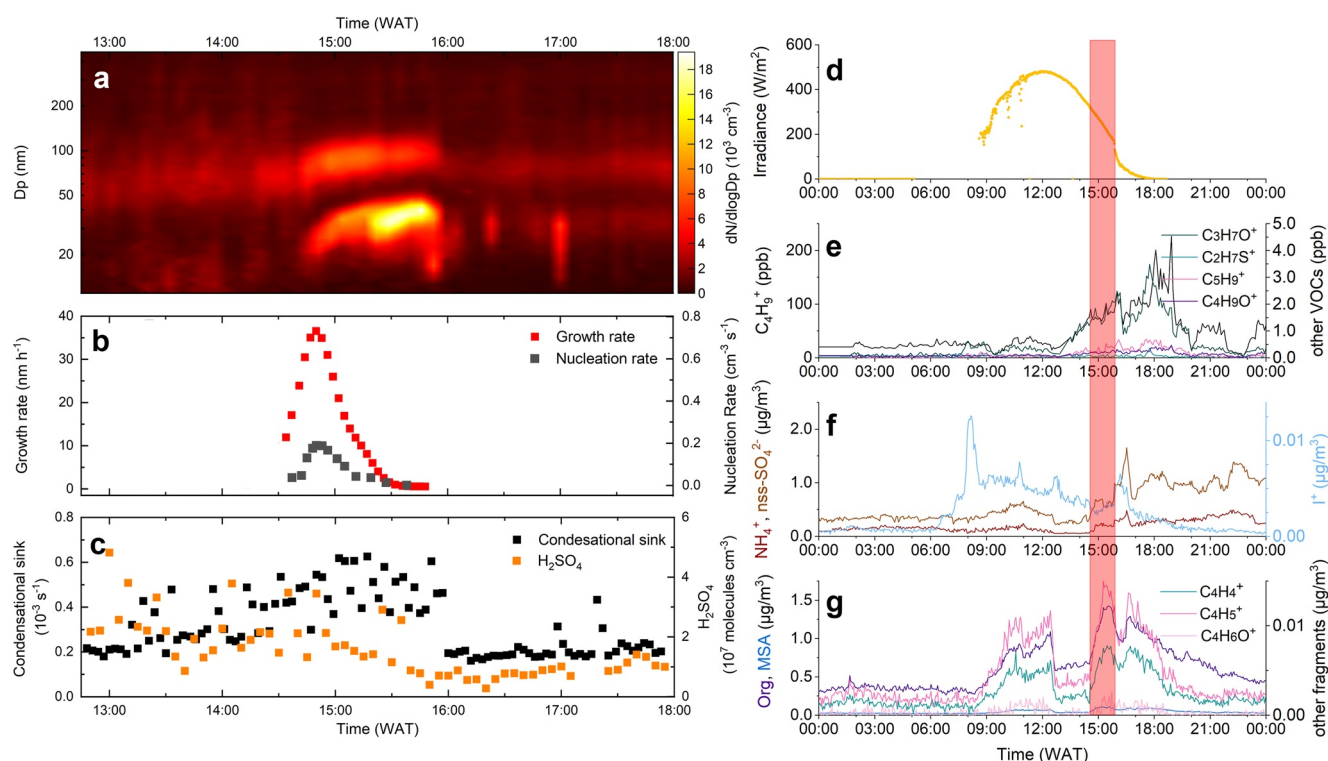


**Figure 3.** Number size distributions (a) measured by the Scanning Mobility Particle Sizer during a new particle formation (NPF) event on 9 September 2017 in Henties Bay (Namibia). Concurrent time-series of the condensational growth rate and the nucleation rate (b). Concurrent time-series of the condensational sink and calculated concentrations of sulphuric acid (c). Diurnal trend of irradiance (d), diurnal trends of gas-phase components ( $C_4H_9^+$  butenes,  $C_3H_7O^+$  acetone,  $C_2H_7S^+$  DMS,  $C_5H_9^+$  isoprene,  $C_4H_9O^+$ , a possible oxidation product of butene) (e), diurnal trends of ammonium, non-sea-salt sulfate and iodine in the particulate phase (f), and diurnal trends of organics (Org), methanesulphonic acid (MSA), and three species/fragments that may be attributed to butene oxidation (g). The red shaded square across all panels on the right indicates the start of the nucleation event of the 9 September 2017, to which all diurnal trends refer. Condensational growth and nucleation rates in panel “b” are shown only for the NPF event starting at around 14h30–15h00. Time is in West Africa Time (WAT) (UTC+1).

VOCs at around 11–13 hr WAT, of which the most abundant was butene. In the case of 9 September, butenes started to increase at around 13h00 WAT, with one of the possible first-generation oxidation products following shortly thereafter (Figure 3). According to the results of the Master Chemical Mechanism (MCM) modeling of butene oxidation (Text S5 in Supporting Information S1), butene oxidation products peaked a couple of hours later, around the time when the nucleation event started. However, while butenes are SOA producers (Derwent et al., 2010), it is unlikely that they produce extremely low volatility compounds that could directly trigger pure organic nucleation. Ozonolysis of butenes could, however, lead to the production of SCIs able to oxidize  $SO_2$  as observed in urban environments (Guo et al., 2020; Yang et al., 2021). Calculated sulfuric acid concentrations (see Section “2.7 Calculation of the atmospheric concentrations of sulfuric acid”) using satellite-retrieved data of surface  $SO_2$  concentrations (median of 50 ppt, interquartile range of 50 ppt, Text S1, Figure S3 in Supporting Information S1), which were in line with previously observed concentrations in the Atlantic Ocean and Namibia (50 ppt–2.5 ppb) (Andreae et al., 1995; Husar et al., 2017; Martins et al., 2007; Sinha et al., 2003) but higher than expected compared with DMS concentrations (the DMS median value was 40 ppt in this campaign, while it was about 10 times higher than  $SO_2$  at other oceanic locations (Ayers et al., 1997; Leck & Persson, 1996)), reached a level around  $6.1 \cdot 10^7$  molecules/cm<sup>3</sup> on the 9 September 2017, peaking about half an hour before the appearance of the new particles (Figure 3). Surprisingly, these concentrations are predominantly due to SCIs reactivity (approximately 75%) compared to OH oxidation of  $SO_2$  despite being in daylight hours. This result can however be explained by the high concentrations of butenes (in the range 70–80 ppb) and  $O_3$  (>20 ppb) around the start of the nucleation event. While SCIs seem to dominate  $SO_2$  oxidation, it is likely that NPF events are triggered by a combination of SCI and OH chemistry, with solar irradiance enhancing both OH production and VOC emissions from the marine biota. The results of the MCM modeling of butene oxidation (Text S5 in Supporting Information S1) also indicate that butene-SOA may contribute to the survival and growth of the newly formed particles.

The hypothesis that butenes may contribute to NPF through SCIs chemistry is further supported by the moderate but statistically significant correlation between the calculated concentrations of  $\text{H}_2\text{SO}_4$  and the nucleation rate ( $r = 0.22$ , not lagged) and the correlation of the time-series of  $\text{C}_3\text{H}_5^+$  (mainly linked to butene fragmentation as identified in the standard) with the time-series of particle number concentration ( $r = 0.467$ ) with a lag time of 100 min (Table S3 in Supporting Information S1). Among the particle component measured in the Aitken and accumulation modes by the c-ToF-AMS, sulfate and iodine are the only species observed that are known to promote NPF. Weak-to-moderate, but statistically significant ( $|r| > 0.033$ ), lagged correlations were obtained between nucleation rates and  $\text{C}_4\text{H}_5\text{O}_2^+$  ( $r = 0.042$ ),  $\text{C}_5\text{H}_3\text{O}_7^+$  ( $r = 0.316$ ),  $\text{C}_6\text{H}_9\text{O}_2^+$  ( $r = 0.219$ ), and  $\text{C}_7\text{H}_{11}\text{O}_4^+$  ( $r = 0.332$ ) measured with PTR-ToF-MS, all with a lag time of 0 min (not lagged). The first ion may be a fragment of an oxidation product of butenes given that it is an oxygenated C4 ion and its correlation with the nucleation rate has a lower lag time compared to the hypothesized parent compound. Correlations between the time-series of particle chemical components measured with a c-ToF-AMS and time-series of particle concentration in number, nucleation rate, condensational growth rate, and CS (Table S4 in Supporting Information S1) supported the hypothesis that butene oxidation may be involved in the coastal formation of new particles. Nucleation rates are correlated with particulate organic fragments with a lagged time ranging from  $-155$  min to  $-180$  min (Table S4 in Supporting Information S1). A negative lag time, which means that particle components are being driven by nucleation rates, reflects the fact that particles need to grow to larger diameters to be detected by the c-ToF-AMS, whose detection efficiency is rather poor below 50 nm (see Section 2.5). Contrarily to previous studies at higher latitudes (Allan et al., 2015; Baccarini et al., 2020; Mäkelä et al., 2002; McFiggans et al., 2010; Wan et al., 2020; Yu et al., 2019), a clear link between iodine species and NPF events was not observed during the AEROCLO-sA campaign (example correlation with the  $\text{I}^+$  fragment measured by the c-ToF-AMS shown in Table S4 in Supporting Information S1). However, NPF event of the 9 September (Figure 3a) occurs hours after a spike of the iodide ion, locally produced in the morning (Figure 3f), which may be driving nucleation even if it is only a minor contributor to aerosol mass at the size range detectable by the c-ToF-AMS. Laminaria kelp species are present in this upwelling system, and they are known for their iodine bioaccumulation and reactive iodine release (McFiggans et al., 2004; Velimirov et al., 1977). In addition, a previous study in the High Arctic, where iodic acid plays a major role in NPF, showed that particle growth was driven by other species, for example, organics (Lawler et al., 2021). Consequently, with the data at hand, we cannot discriminate between these two competing hypotheses (i.e., iodine vs. sulfuric acid triggered nucleation).

Unlike previous studies, which associated NPF events to the entrainment of particles formed in the free troposphere (Kerminen et al., 2018) or NPF events occurring at the top of the marine boundary layer close to the stratocumulus cloud deck (Zheng et al., 2021), here we show that NPF events can occur within the marine boundary layer in highly productive coastal ecosystems. In this campaign, entrainment of particles from the free troposphere can be excluded as long-range transport of biomass burning aerosol was observed in the free troposphere during the campaign (Chazette et al., 2019; Formenti et al., 2019), but no evidence of biomass burning reaching the ground-based site was observed from VOCs (such as acetonitrile) and aerosol composition measurements. This is in agreement with previous findings in Henties Bay (Formenti et al., 2018; Klopper et al., 2020) and with other studies (Haywood et al., 2021; Redemann et al., 2021; Zuidema et al., 2018), which showed that during the austral spring the entrainment of biomass burning emissions in the marine boundary layer occurs well offshore of the subcontinent over the central southern Atlantic Ocean. The NPF events occurring at the stratocumulus cloud deck could rather contribute to the increase in particle number concentrations observed in the Aitken mode (Figure 3). Secondary aerosol components, such as non-sea-salt sulfate, do not show any relation with NPF but are rather linked to condensational growth and increase in particle number concentrations for larger particle sizes (Table S4 in Supporting Information S1). While the c-ToF-AMS cannot inform us on the early stages of NPF events, it shows that growth of these newly formed particles involves not only sulfate but also organic compounds (period highlighted in red in Figure 3). These organic compounds are likely to be produced, at least in part, by photooxidation of butenes, given the high concentrations of the parent compounds and their ability to produce SOA (Derwent et al., 2010).

#### 4. Conclusions

We have demonstrated that the Benguela ecosystem is a large emitter of reactive VOCs, especially butenes, which may oxidize  $\text{SO}_2$  to  $\text{H}_2\text{SO}_4$  through SCIs chemistry and may be contributing to NPF events within the marine boundary layer. While emissions of non-methane VOCs are considered in global modeling studies as drivers of

greenhouse gas lifetimes and concentrations (IPCC, 2021), our study shows that emission factors of butenes need to be revisited. The Benguela ecosystem alone may act as an important driver of regional climate. However, if similarly productive coastal environments, for which data are not yet available, are strong emitters of butenes such emissions will have global impacts. Concerning aerosol production, organic photochemistry is not considered at all in climate models as it is computationally expensive. Efforts are being made to include the chemistry of DMS from marine biogenic emissions as it has been recognised as important for the Earth's climate being an efficient aerosol and cloud droplet producer (Fung et al., 2022; Grandey & Wang, 2015; Mayer et al., 2020; Novak et al., 2021). We showed that butenes may also contribute to marine NPF, deserving a place in climate models that currently account for “unknown organic emissions” with a scaling factor applied to DMS emissions (Bodas-Salcedo et al., 2019; Mulcahy et al., 2018). According to our observation, butenes can be found at concentrations at least three orders of magnitude larger than DMS in highly productive coastal environments and thus their climatic impact requires investigation.

### Conflict of Interest

The authors declare no conflicts of interest relevant to this study.

### Data Availability Statement

All data are made freely available by the French national service for atmospheric data AERIS-SEDOO data at <https://baobab.sedoo.fr/AEROCLO/>.

### Acknowledgments

Authors are grateful to Dr Vijay Kanawade and Dr Bart Verheggen for assistance with the calculations of condensational growth rates and nucleation rates and with the use of the PARGAN codes. The authors wish to thank Edouard Panguì (LISA) for his technical support during the field campaign preparation and AERIS (<https://www.aeris-data.fr/>), the French centre for atmospheric data and service, for providing the campaign website and organising the curation and open distribution of Aerosols, Radiation and Clouds in southern Africa (AEROCLO-sA) data. Authors are grateful to the AEROCLO-sA consortium for their work in the field and during the preparation of the field campaign, and Sam Nujoma Marine and Coastal Resources Research Centre for hosting the field campaign. This work was supported by the French National Research Agency under grant agreement no ANR-15-CE01-0014-01, the French national programme LEFE/INSU, the French National Agency for Space Studies (CNES), and the South African National Research Foundation (NRF) under grant UID 105958. DF's work was supported by the Supporting TAleNT in ReSearch@University of Padova STARS-StG “MOCAA” and MIUR-PRIN-2017 “AMICO” awarded to CG. The GEOS data used in this study have been provided by the Global Modeling and Assimilation Office (GMAO) at NASA Goddard Space Flight Center through the online data portal in the NASA Center for Climate Simulation.

### References

- Achyuthan, K. E., Harper, J. C., Manginell, R. P., & Moorman, M. W. (2017). Volatile metabolites emission by in vivo microalgae—An overlooked opportunity? *Metabolites*, 7(3), 39. <https://doi.org/10.3390/metabo7030039>
- Ali, G. (2004). Identification of volatile organic compounds produced by algae. *Egyptian Journal of Phycology*, 5(1), 71–81. Retrieved from <https://www.ejmanager.com/mnstemp/167/167-1466514723.pdf>
- Allan, J. D., Williams, P. I., Najera, J., Whitehead, J. D., Flynn, M. J., Taylor, J. W., et al. (2015). Iodine observed in new particle formation events in the Arctic atmosphere during ACCACIA. *Atmospheric Chemistry and Physics*, 15(10), 5599–5609. <https://doi.org/10.5194/acp-15-5599-2015>
- Andreae, M. O., Elbert, W., & deMora, S. J. (1995). Biogenic sulfur emissions and aerosols over the tropical South Atlantic: 3. Atmospheric dimethylsulfide, aerosols and cloud condensation nuclei. *Journal of Geophysical Research*, 100(D6), 11335. <https://doi.org/10.1029/94JD02828>
- Arnold, S. R., Spracklen, D. V., Williams, J., Yassaa, N., Sciare, J., Bonsang, B., et al. (2009). Evaluation of the global oceanic isoprene source and its impacts on marine organic carbon aerosol. *Atmospheric Chemistry and Physics*, 9(4), 1253–1262. <https://doi.org/10.5194/acp-9-1253-2009>
- Ayers, G. P., Caine, J. M., Gillett, R. W., Saltzman, E. S., & Hooper, M. (1997). Sulfur dioxide and dimethyl sulphide in marine air at Cape Grim, Tasmania. *Tellus B: Chemical and Physical Meteorology*, 49(3), 292–299. <https://doi.org/10.3402/tellusb.v49i3.15968>
- Baccarini, A., Karlsson, L., Dommen, J., Duplessis, P., Vüllers, J., Brooks, I. M., et al. (2020). Frequent new particle formation over the high Arctic pack ice by enhanced iodine emissions. *Nature Communications*, 11(1), 1–11. <https://doi.org/10.1038/s41467-020-18551-0>
- Blauw, A. N., Los, F. J., Huisman, J., & Peperzak, L. (2010). Nuisance foam events and Phaeocystis globosa blooms in Dutch coastal waters analyzed with fuzzy logic. *Journal of Marine Systems*, 83(3–4), 115–126. <https://doi.org/10.1016/j.jmarsys.2010.05.003>
- Bodas-Salcedo, A., Mulcahy, J. P., Andrews, T., Williams, K. D., Ringer, M. A., Field, P. R., & Elsaesser, G. S. (2019). Strong dependence of atmospheric feedbacks on mixed-phase microphysics and aerosol-cloud interactions in HadGEM3. *Journal of Advances in Modeling Earth Systems*, 11(6), 1735–1758. <https://doi.org/10.1029/2019MS001688>
- Bonsang, B., & Lambert, G. (1985). Nonmethane hydrocarbons in an oceanic atmosphere. *Journal of Atmospheric Chemistry*, 2(3), 257–271. <https://doi.org/10.1007/BF00051076>
- Bourtsoukidis, E., Ernle, L., Crowley, J. N., Lelieveld, J., Paris, J. D., Pozzer, A., et al. (2019). Non-methane hydrocarbon (C2-C8) sources and sinks around the Arabian Peninsula. *Atmospheric Chemistry and Physics*, 19(10), 7209–7232. <https://doi.org/10.5194/acp-19-7209-2019>
- Brean, J., Dall'Osto, M., Simó, R., Shi, Z., Beddows, D. C. S., & Harrison, R. M. (2021). Open ocean and coastal new particle formation from sulfuric acid and amines around the Antarctic Peninsula. *Nature Geoscience*, 14(6), 383–388. <https://doi.org/10.1038/s41561-021-00751-y>
- Brooks, S. D., & Thornton, D. C. O. (2018). Marine aerosols and clouds. *Annual Review of Marine Science*, 10(1), 289–313. <https://doi.org/10.1146/annurev-marine-121916-063148>
- Brussaard, C. P. D. (2004). Optimization of procedures for counting viruses by flow cytometry. *Applied and Environmental Microbiology*, 70(3), 1506–1513. <https://doi.org/10.1128/AEM.70.3.1506-1513.2004>
- CDS. (2021). Copernicus Climate Change Service (C3S): Ocean colour daily data from 1997 to present derived from satellite observations. Accessed 18 May 2021. Retrieved from <https://cds.climate.copernicus.eu/cdsapp#!/home/>
- Charlson, R. J., Lovelock, J. E., Andreae, M. O., & Warren, S. G. (1987). Oceanic phytoplankton, atmospheric sulphur, cloud. *Nature*, 330(6148), 1987. <https://doi.org/10.1038/33052660>
- Chazette, P., Flamant, C., Totems, J., Gaetani, M., Smith, G., Baron, A., et al. (2019). Evidence of the complexity of aerosol transport in the lower troposphere on the Namibian coast during AEROCLO-sA. *Atmospheric Chemistry and Physics Discussions*, 19(23), 14979–15005. <https://doi.org/10.5194/acp-19-14979-2019>
- Clarke, A. D., Davis, D., Kapustin, V. N., Eisele, F., Chen, G., Paluch, I., et al. (1998). Particle nucleation in the tropical boundary layer and its coupling to marine sulfur sources. *Science*, 282(5386), 89–92. <https://doi.org/10.1126/science.282.5386.89>
- Cohen, J. (1988). *Statistical power analysis for the behavioral sciences*. Lawrence Erlbaum Associates Inc.

- Colomb, A., Yassaa, N., Williams, J., Peeken, I., & Lochte, K. (2008). Screening volatile organic compounds (VOCs) emissions from five marine phytoplankton species by head space gas chromatography/mass spectrometry (HS-GC/MS). *Journal of Environmental Monitoring*, *10*(3), 325–330. <https://doi.org/10.1039/b715312k>
- Dal Maso, M., Kulmala, M., Lehtinen, K. E. J., Mkelä, J. M., Aalto, P., & O'Dowd, C. D. (2002). Condensation and coagulation sinks and formation of nucleation mode particles in coastal and boreal forest boundary layers. *Journal of Geophysical Research*, *107*(19). <https://doi.org/10.1029/2001JD001053>
- Danovaro, R., Corinaldesi, C., Dell'Anno, A., Fuhrman, J. A., Middelburg, J. J., Noble, R. T., & Suttle, C. A. (2011). Marine viruses and global climate change. *FEMS Microbiology Reviews*, *35*(6), 993–1034. <https://doi.org/10.1111/j.1574-6976.2010.00258.x>
- DeCarlo, P. F., Slowik, J. G., Worsnop, D. R., Davidovits, P., & Jimenez, J. L. (2004). Particle morphology and density characterization by combined mobility and aerodynamic diameter measurements. Part 1: Theory. *Aerosol Science and Technology*, *38*(12), 1185–1205. <https://doi.org/10.1080/027868290903907>
- Derwent, R. G. (2007). Sources, distributions, and fates of VOCs in the atmosphere. *Volatile Organic Compounds in the Atmosphere*, (23), 1–16. <https://doi.org/10.1039/9781847552310-00001>
- Derwent, R. G., Jenkin, M. E., Utembe, S. R., Shallcross, D. E., Murrells, T. P., & Passant, N. R. (2010). Secondary organic aerosol formation from a large number of reactive man-made organic compounds. *The Science of the Total Environment*, *408*(16), 3374–3381. <https://doi.org/10.1016/j.scitotenv.2010.04.013>
- Donahue, N. M., & Prinn, R. G. (1993). In situ nonmethane hydrocarbon measurements on SAGA 3. *Journal of Geophysical Research*, *98*(D9), 16915. <https://doi.org/10.1029/93JD01780>
- Duncanu, M., David, M., Kartigeyane, S., Cirtog, M., Doussin, J., & Picquet-Varrault, B. (2017). Measurement of alkyl and multifunctional organic nitrates by proton-transfer-reaction mass spectrometry. *Atmospheric Measurement Techniques*, *10*(4), 1445–1463. <https://doi.org/10.5194/amt-10-1445-2017>
- Ellis, A. M., & Mayhew, C. A. (2014). *Proton transfer reaction mass spectrometry: Principles and applications*. John Wiley & Sons, Ltd.
- Formenti, P., D'Anna, B., Flamant, C., Mallet, M., Piketh, S. J., Schepanski, K., et al. (2019). The Aerosols, Radiation and Clouds in Southern Africa field campaign in Namibia: Overview, Illustrative Observations, and way forward. *Bulletin of the American Meteorological Society*, *100*(7), 1277–1298. <https://doi.org/10.1175/BAMS-D-17-0278.1>
- Formenti, P., John Piketh, S., Namwoonde, A., Klopper, D., Burger, R., Cazaunau, M., et al. (2018). Three years of measurements of light-absorbing aerosols over coastal Namibia: Seasonality, origin, and transport. *Atmospheric Chemistry and Physics*, *18*(23), 17003–17016. <https://doi.org/10.5194/acp-18-17003-2018>
- Fung, K. M., Heald, C. L., Kroll, J. H., Wang, S., Jo, D. S., Gettelman, A., et al. (2022). Exploring dimethyl sulfide (DMS) oxidation and implications for global aerosol radiative forcing. *Atmospheric Chemistry and Physics*, *22*(2), 1549–1573. <https://doi.org/10.5194/acp-22-1549-2022>
- Gantt, S. E., McMurray, S. E., Stubler, A. D., Finelli, C. M., Pawlik, J. R., & Erwin, P. M. (2019). Testing the relationship between microbiome composition and flux of carbon and nutrients in Caribbean coral reef sponges. *Microbiome*, *7*(1), 1–13. <https://doi.org/10.1186/s40168-019-0739-x>
- Geyh, M. A., & Ploethner, D. (1995). *Groundwater isotope study in the Omaruru River delta aquifer, central Namib desert, Namibia Application of Tracers in Arid Zone Hydrology (Proceedings of the Vienna Symposium, August 1994)*. IAHS Publications. no. 232.
- Grandey, B. S., & Wang, C. (2015). Enhanced marine sulphur emissions offset global warming and impact rainfall. *Scientific Reports*, *5*, 1–7. <https://doi.org/10.1038/srep13055>
- Guo, Y., Yan, C., Li, C., Feng, Z., Zhou, Y., Lin, Z., et al. (2020). Formation of nighttime sulfuric acid from the ozonolysis of alkenes in Beijing. *Atmospheric Chemistry and Physics Discussions*, 1–18. <https://doi.org/10.5194/acp-2019-1111>
- Halsey, K. H., Giovannoni, S. J., Graus, M., Zhao, Y., Landry, Z., Thrash, J. C., et al. (2017). Biological cycling of volatile organic carbon by phytoplankton and bacterioplankton. *Limnology & Oceanography*, *62*(6), 2650–2661. <https://doi.org/10.1002/lno.10596>
- Hansen, A., Ohde, T., & Wasmund, N. (2014). Succession of micro- and nanoplankton groups in ageing upwelled waters off Namibia. *Journal of Marine Systems*, *140*, 130–137. <https://doi.org/10.1016/j.jmarsys.2014.05.003>
- Haywood, J. M., Abel, S. J., Barrett, P. A., Bellouin, N., Blyth, A., Bower, K. N., et al. (2021). The CLoud-Aerosol-Radiation interaction and forcing: Year 2017 (CLARIFY-2017) measurement campaign. *Atmospheric Chemistry and Physics*, *21*(2), 1049–1084. <https://doi.org/10.5194/acp-21-1049-2021>
- Hinds, W. C. (1999). *Aerosol technology: Properties, behavior, and measurement of airborne particles* (2nd ed.). John Wiley & Sons, Ltd.
- Husar, R. B., Lodge, J. P., & Moore, D. J. (2017). *Sulfur in the Atmosphere: Proceedings of the International Symposium Held in Dubrovnik, Yugoslavia, 7–14 September 1977*. Elsevier Science. Retrieved from <https://books.google.co.uk/books?id=EvsbBQAAQBAJ>
- IPCC. (2021). *Climate Change 2021: The Physical Science Basis. Contribution of Working Group I to the Sixth Assessment Report of the Intergovernmental Panel on Climate Change*. In V. Masson-Delmotte, P. Zhai, A. Pirani, S. L. Connors, C. Péan, S. Berger, et al. (Eds.), Cambridge University Press. Retrieved from <https://www.ipcc.ch/report/ar6/wg1/>
- Jerković, I., Marijanović, Z., Roje, M., Kus, P. M., Jokić, S., & Čož-Rakovac, R. (2018). Phytochemical study of the headspace volatile organic compounds of fresh algae and seagrass from the Adriatic Sea (single point collection). *PLoS One*, *13*(5), 1–13. <https://doi.org/10.1371/journal.pone.0196462>
- Kerminen, V. M., Chen, X., Vakkari, V., Petäjä, T., Kulmala, M., & Bianchi, F. (2018). Atmospheric new particle formation and growth: Review of field observations. *Environmental Research Letters*, *13*(10). <https://doi.org/10.1088/1748-9326/aadf3c>
- Klopper, D., Formenti, P., Namwoonde, A., Cazaunau, M., Chevaillier, S., Feron, A., et al. (2020). Chemical composition and source apportionment of atmospheric aerosols on the Namibian coast. *Atmospheric Chemistry and Physics*, *20*(24), 1–43. <https://doi.org/10.5194/acp-2020-388>
- Korpi, A., Järnberg, J., & Pasanen, A. L. (2009). Microbial volatile organic compounds. *Critical Reviews in Toxicology*, *39*(2), 139–193. <https://doi.org/10.1080/10408440802291497>
- Kulmala, M., Dada, L., Daellenbach, K. R., Yan, C., Stolzenburg, D., Kontkanen, J., et al. (2021). Is reducing new particle formation a plausible solution to mitigate particulate air pollution in Beijing and other Chinese megacities? *Faraday Discussions*, *226*, 334–347. <https://doi.org/10.1039/d0fd00078g>
- Kulmala, M., Kerminen, V. M., Petäjä, T., Ding, A. J., & Wang, L. (2017). Atmospheric gas-to-particle conversion: Why NPF events are observed in megacities? *Faraday Discussions*, *200*, 271–288. <https://doi.org/10.1039/c6fd00257a>
- Lamont, T., Barlow, R. G., & Brewin, R. J. W. (2019). Long-Term Trends in Phytoplankton Chlorophyll a and Size Structure in the Benguela Upwelling System. *Journal of Geophysical Research: Oceans*, *124*(2), 1170–1195. <https://doi.org/10.1029/2018JC014334>
- Lawler, M. J., Saltzman, E. S., Karlsson, L., Zieger, P., Salter, M., Baccarini, A., et al. (2021). New insights into the composition and origins of ultrafine aerosol in the summertime high Arctic. *Geophysical Research Letters*, *48*(21), 1–11. <https://doi.org/10.1029/2021GL094395>

- Lea-Smith, D. J., Biller, S. J., Davey, M. P., Cotton, C. A. R., Sepulveda, B. M. P., Turchyn, A. V., et al. (2015). Contribution of cyanobacterial alkane production to the ocean hydrocarbon cycle. *Proceedings of the National Academy of Sciences of the United States of America*, *112*(44), 13591–13596. <https://doi.org/10.1073/pnas.1507274112>
- Lebaron, P., Servais, P., Agogue, H., Courties, C., & Joux, F. (2001). Does the high nucleic acid content of individual bacterial cells allow us to discriminate between active cells and inactive cells in aquatic systems? *Applied and Environmental Microbiology*, *67*(4), 1775–1782. <https://doi.org/10.1128/AEM.67.4.1775-1782.2001>
- Leck, C., & Persson, C. (1996). Seasonal and short-term variability in dimethyl sulfide, sulfur dioxide and biogenic sulfur and sea salt aerosol particles in the arctic marine boundary layer during summer and autumn. *Tellus Series B Chemical and Physical Meteorology*, *48*(2), 272–299. <https://doi.org/10.3402/tellusb.v48i2.15891>
- Lewis, A. C., Hopkins, J. R., Carpenter, L. J., Stanton, J., Read, K. A., & Pilling, M. J. (2005). Sources and sinks of acetone, methanol, and acetaldehyde in North Atlantic air. *Atmospheric Chemistry and Physics Discussions*, *5*(2), 1285–1317. <https://doi.org/10.5194/acpd-5-1285-2005>
- Lin, Y. H., Knipping, E. M., Edgerton, E. S., Shaw, S. L., & Surratt, J. D. (2013). Investigating the influences of SO<sub>2</sub> and NH<sub>3</sub> levels on isoprene-derived secondary organic aerosol formation using conditional sampling approaches. *Atmospheric Chemistry and Physics*, *13*(16), 8457–8470. <https://doi.org/10.5194/acp-13-8457-2013>
- Liu, P. S. K., Deng, R., Smith, K. A., Williams, L. R., Jayne, J. T., Canagaratna, M. R., et al. (2007). Transmission efficiency of an aerodynamic focusing lens system: Comparison of model calculations and laboratory measurements for the aerodyne aerosol mass spectrometer. *Aerosol Science and Technology*, *41*(8), 721–733. <https://doi.org/10.1080/02786820701422278>
- Mäkelä, J. M., Hoffmann, T., Holzke, C., Väkevä, M., Suni, T., Mattila, T., et al. (2002). Biogenic iodine emissions and identification of end-products in coastal ultrafine particles during nucleation bursts. *Journal of Geophysical Research*, *107*(19), 1–14. <https://doi.org/10.1029/2001JD000580>
- Martins, J. J., Dhammapala, R. S., Lachmann, G., Galy-Lacaux, C., & Pienaar, J. J. (2007). Long-term measurements of sulphur dioxide, nitrogen dioxide, ammonia, nitric acid and ozone in southern Africa using passive samplers. *South African Journal of Science*, *103*(7–8), 336–342. <https://doi.org/10.5194/acpd-10-4407-2010>
- Mayer, K. J., Wang, X., Santander, M. V., Mitts, B. A., Sauer, J. S., Sultana, C. M., et al. (2020). Secondary marine aerosol plays a dominant role over primary sea spray aerosol in cloud formation. *ACS Central Science*, *6*(12), 2259–2266. <https://doi.org/10.1021/acscentsci.0c00793>
- McFiggans, G., Bale, C. S. E., Ball, S. M., Beames, J. M., Bloss, W. J., Carpenter, L. J., et al. (2010). Iodine-mediated coastal particle formation: An overview of the Reactive Halogens in the Marine boundary layer (RHAMBLE) Roscoff coastal study. *Atmospheric Chemistry and Physics*, *10*(6), 2975–2999. <https://doi.org/10.5194/acp-10-2975-2010>
- McFiggans, G., Coe, H., Burgess, R., Allan, J., Cubison, M., Alfarra, M. R., et al. (2004). Direct evidence for coastal iodine particles from *Laminaria* macroalgae – Linkage to emissions of molecular iodine. *Atmospheric Chemistry and Physics*, *4*(3), 701–713. <https://doi.org/10.5194/acp-4-701-2004>
- McKay, W., Turner, M. F., Jones, B. M. R., & Halliwell, C. M. (1996). Emissions of hydrocarbons from marine phytoplankton – Some results from controlled laboratory experiments. *Atmospheric Environment*, *30*(14), 2583–2593.
- Mikkonen, S., Romakkaniemi, S., Smith, J. N., Korhonen, H., Petäjä, T., Plass-Dümler, C., et al. (2011). A statistical proxy for sulphuric acid concentration. *Atmospheric Chemistry and Physics*, *11*(21), 11319–11334. <https://doi.org/10.5194/acp-11-11319-2011>
- Misztal, P. K., Lymperopoulou, D. S., Adams, R., Scott, R., Lindow, S., Bruns, T., et al. (2018). *Emission factors of microbial volatile organic compounds from environmental bacteria and fungi*. Environmental Science & Technology. <https://doi.org/10.1021/acs.est.8b00806>
- Mulcahy, J. P., Jones, C., Sellar, A., Johnson, B., Boutle, I. A., Jones, A., et al. (2018). Improved aerosol processes and effective radiative forcing in HadGEM3 and UKESM1. *Journal of Advances in Modeling Earth Systems*, *10*(11), 2786–2805. <https://doi.org/10.1029/2018MS001464>
- Müller, M., George, C., & D'Anna, B. (2011). Enhanced spectral analysis of C-TOF Aerosol Mass Spectrometer data: Iterative residual analysis and cumulative peak fitting. *International Journal of Mass Spectrometry*, *306*(1), 1–8. <https://doi.org/10.1016/j.ijms.2011.04.007>
- Novak, G. A., Fite, C. H., Holmes, C. D., Veres, P. R., Neuman, J. A., Faloon, I., et al. (2021). Rapid cloud removal of dimethyl sulfide oxidation products limits SO<sub>2</sub> and cloud condensation nuclei production in the marine atmosphere. *Proceedings of the National Academy of Sciences*, *118*. <https://doi.org/10.1073/pnas.2110472118>
- Nuccio, J., Seaton, P. J., & Kieber, R. J. (1995). Biological production of formaldehyde in the marine environment. *Limnology & Oceanography*, *40*(3), 521–527. <https://doi.org/10.4319/lo.1995.40.3.0521>
- O'Dowd, C., Ceburnis, D., Ovadnevaite, J., Bialek, J., Stengel, D. B., Zacharias, M., et al. (2015). Connecting marine productivity to sea-spray via nanoscale biological processes: Phytoplankton Dance or Death Disco? *Scientific Reports*, *5*(September), 1–11. <https://doi.org/10.1038/srep14883>
- Ohde, T., & Dadou, I. (2018). Seasonal and annual variability of coastal sulphur plumes in the northern Benguela upwelling system. *PLoS One*, *13*(2), e0192140. <https://doi.org/10.1371/journal.pone.0192140>
- Papaleo, M. C., Romoli, R., Bartolucci, G., Maida, I., Perrin, E., Fondi, M., et al. (2013). Bioactive volatile organic compounds from Antarctic (sponges) bacteria. *New Biotechnology*, *30*(6), 824–838. <https://doi.org/10.1016/j.nbt.2013.03.011>
- Pecqueur, D., Vidussi, F., Fouilland, E., Le Floch, E., Mas, S., Roques, C., et al. (2011). Dynamics of microbial planktonic food web components during a river flash flood in a Mediterranean coastal lagoon. *Hydrobiologia*, *673*(1), 13–27. <https://doi.org/10.1007/s10750-011-0745-x>
- Pirjola, L., O'Dowd, C. D., Brooks, I. M., & Kulmala, M. (2000). Can new particle formation occur in the clean marine boundary layer? *Journal of Geophysical Research*, *105*(D21), 26531–26546. <https://doi.org/10.1029/2000JD900310>
- Quinn, P. K., & Bates, T. S. (2011). The case against climate regulation via oceanic phytoplankton sulphur emissions. *Nature*, *480*(7375), 51–56. <https://doi.org/10.1038/nature10580>
- Rahlff, J., Stolle, C., Giebel, H.-A., Mustaffa, N. I. H., Wurl, O., & PR Herlemann, D. (2020). Sea foams are ephemeral hotspots for distinctive bacterial communities contrasting sea-surface microlayer and underlying surface water. *BioRxiv*, 820696. <https://doi.org/10.1101/820696>
- Rajot, J. L., Formenti, P., Alfaro, S., Desboeufs, K., Chevaillier, S., Chatenet, B., et al. (2008). AMMA dust experiment: An overview of measurements performed during the dry season special observation period (SOP0) at the Banizoumbou (Niger) supersite. *Journal of Geophysical Research*, *113*(23), 1–18. <https://doi.org/10.1029/2008JD009906>
- Ratte, M., Plass-Dümler, C., Koppmann, R., & Rudolph, J. (1995). Horizontal and vertical profiles of light hydrocarbons in sea water related to biological, chemical and physical parameters. *Tellus B: Chemical and Physical Meteorology*, *47*(5), 607–623. <https://doi.org/10.3402/tellusb.v47i5.16076>
- Redemann, J., Wood, R., Zuidema, P., Doherty, S. J., Luna, B., LeBlanc, S. E., et al. (2021). An overview of the ORACLES (ObseRvations of aerosols above CLOUDs and their intERactionS) project: Aerosol-cloud-radiation interactions in the southeast Atlantic basin. *Atmospheric Chemistry and Physics*, *21*(3), 1507–1563. <https://doi.org/10.5194/acp-21-1507-2021>
- Rocco, M., Dunne, E., Peltola, M., Barr, N., Williams, J., Colomb, A., et al. (2021). Oceanic phytoplankton are a potentially important source of benzenoids to the remote marine atmosphere. *Communications Earth & Environment*, *2*(1), 1–8. <https://doi.org/10.1038/s43247-021-00253-0>

- Roveillo, Q., Dervaux, J., Wang, Y., Rouyer, F., Zanchi, D., Seuront, L., & Elias, F. (2020). Trapping of swimming microalgae in foam. *Journal of The Royal Society Interface*, *17*(168). <https://doi.org/10.1098/rsif.2020.0077rsif20200077>
- Russell, L. M., Pandis, S. N., & Seinfeld, J. H. (1994). Aerosol production and growth in the marine boundary layer. *Journal of Geophysical Research*, *99*(D10). <https://doi.org/10.1029/94jd01932>
- Saliba, G., Chen, C. L., Lewis, S., Russell, L. M., Quinn, P. K., Bates, T. S., et al. (2020). Seasonal differences and variability of concentrations, chemical composition, and cloud condensation nuclei of marine aerosol over the North Atlantic. *Journal of Geophysical Research: Atmospheres*, *125*(19). <https://doi.org/10.1029/2020JD033145>
- Schilling, K., & Zessner, M. (2011). Foam in the aquatic environment. *Water Research*, *45*(15), 4355–4366. <https://doi.org/10.1016/j.watres.2011.06.004>
- Schneider, S. R., Collins, D. B., Lim, C. Y., Zhu, L., & Abbott, J. P. D. (2019). Formation of Secondary Organic Aerosol from the Heterogeneous Oxidation by Ozone of a Phytoplankton Culture. *ACS Earth and Space Chemistry*, *3*(10), 2298–2306. <https://doi.org/10.1021/acsearthspacechem.9b00201>
- Sharma, U. K., Kajii, Y., & Akimoto, H. (2000). Measurement of NMHCs at Oki Island, Japan: An evidence of long range transport. *Geophysical Research Letters*, *27*(16), 2505–2508. <https://doi.org/10.1029/2000GL011500>
- Shaw, S. L., Gantt, B., & Meskhidze, N. (2010). Production and Emissions of Marine Isoprene and Monoterpenes: A Review. *Advances in Meteorology*, *2010*(1), 1–24. <https://doi.org/10.1155/2010/408696>
- Sinha, P., Hobbs, P. V., Yokelson, R. J., Blake, D. R., Gao, S., & Kirchstetter, T. W. (2003). Distributions of trace gases and aerosols during the dry biomass burning season in southern Africa. *Journal of Geophysical Research*, *108*(17), 1–23. <https://doi.org/10.1029/2003jd003691>
- Swan, H. B., Crough, R. W., Vaattovaara, P., Jones, G. B., Deschaseaux, E. S. M., Eyre, B. D., et al. (2016). Dimethyl sulfide and other biogenic volatile organic compound emissions from branching coral and reef seawater: Potential sources of secondary aerosol over the Great Barrier Reef. *Journal of Atmospheric Chemistry*, *73*(3), 303–328. <https://doi.org/10.1007/s10874-016-9327-7>
- Tournadre, J. (2014). Anthropogenic pressure on the open ocean: The growth of ship traffic revealed by altimeter data analysis. *Geophysical Research Letters*, *41*, 7924–7932. <https://doi.org/10.1002/2014GL061786>
- Tripathi, N., Sahu, L. K., Singh, A., Yadav, R., Patel, A., Patel, K., & Meenu, P. (2020). Elevated levels of biogenic nonmethane hydrocarbons in the marine boundary layer of the Arabian Sea during the intermonsoon. *Journal of Geophysical Research: Atmospheres*, *125*(22), 20–30. <https://doi.org/10.1029/2020JD032869>
- Trueblood, J. V., Wang, X., Or, V. W., Alves, M. R., Santander, M. V., Prather, K. A., & Grassian, V. H. (2019). The old and the new: Aging of sea spray aerosol and formation of secondary marine aerosol through OH oxidation reactions. *ACS Earth and Space Chemistry*, *3*(10), 2307–2314. <https://doi.org/10.1021/acsearthspacechem.9b00087>
- Vaattovaara, P., Huttunen, P. E., Yoon, Y. J., Joutsensaari, J., Lehtinen, K. E. J., O'Dowd, C. D., & Laaksonen, A. (2006). The composition of nucleation and Aitken modes particles during coastal nucleation events: Evidence for marine secondary organic contribution. *Atmospheric Chemistry and Physics*, *6*(12), 4601–4616. <https://doi.org/10.5194/acp-6-4601-2006>
- Velimirov, B., Field, J. G., Griffiths, C. L., & Zoutendyk, P. (1977). The ecology of kelp bed communities in the Benguela upwelling system - Analysis of biomass and spatial distribution. *Helgoländer Wissenschaftliche Meeresuntersuchungen*, *30*(1–4), 495–518. <https://doi.org/10.1007/BF02207857>
- Verheggen, B., & Mozurkewich, M. (2006). An inverse modeling procedure to determine particle growth and nucleation rates from measured aerosol size distributions. *Atmospheric Chemistry and Physics*, *6*(10), 2927–2942. <https://doi.org/10.5194/acp-6-2927-2006>
- Von Der Weiden, S. L., Drewnick, F., & Borrmann, S. (2009). Particle Loss Calculator - A new software tool for the assessment of the performance of aerosol inlet systems. *Atmospheric Measurement Techniques*, *2*(2), 479–494. <https://doi.org/10.5194/amt-2-479-2009>
- Wan, Y., Huang, X., Jiang, B., Kuang, B., Lin, M., Xia, D., et al. (2020). Probing key organic substances driving new particle growth initiated by iodine nucleation in coastal atmosphere. *Atmospheric Chemistry and Physics*, *20*(16), 9821–9835. <https://doi.org/10.5194/acp-20-9821-2020>
- Waterbury, J. B., Watson, S. W., Guillard, R. R. L., & Brand, L. E. (1979). Widespread occurrence of a unicellular, marine, planktonic, cyanobacterium. *Nature*, *277*(5694), 293–294. <https://doi.org/10.1038/277293a0>
- Weber, T., Wiseman, N. A., & Kock, A. (2019). Global ocean methane emissions dominated by shallow coastal waters. *Nature Communications*, *10*(1), 1–10. <https://doi.org/10.1038/s41467-019-12541-7>
- Wendisch, M., & Brenguier, J.-L. (Eds.). (2013). *Airborne Measurements for Environmental Research*. Wiley-VCH Verlag GmbH & Co. KGaA. <https://doi.org/10.1002/9783527653218>
- Yang, L., Nie, W., Liu, Y., Xu, Z., Xiao, M., Qi, X., et al. (2021). Toward Building a Physical Proxy for Gas-Phase Sulfuric Acid Concentration Based on Its Budget Analysis in Polluted Yangtze River Delta, East China. *Environmental Science and Technology*. <https://doi.org/10.1021/acs.est.1c00738>
- Yu, H., Ren, L., Huang, X., Xie, M., He, J., & Xiao, H. (2019). Iodine speciation and size distribution in ambient aerosols at a coastal new particle formation hotspot in China. *Atmospheric Chemistry and Physics*, *19*(6), 4025–4039. <https://doi.org/10.5194/acp-19-4025-2019>
- Zheng, G., Wang, Y., Wood, R., Jensen, M. P., Kuang, C., McCoy, I. L., et al. (2021). New particle formation in the remote marine boundary layer. *Nature Communications*, *12*(1), 527. <https://doi.org/10.1038/s41467-020-20773-1>
- Zuidema, P., Sedlacek, A. J., Flynn, C., Springston, S., Delgado, R., Zhang, J., et al. (2018). The Ascension Island boundary layer in the remote southeast Atlantic is often smoky. *Geophysical Research Letters*, *45*(9), 4456–4465. <https://doi.org/10.1002/2017GL076926>

## References From the Supporting Information

- Andreae, T. W., Andreae, M. O., & Schebeske, G. (1994). Biogenic sulfur emissions and aerosols over the tropical South Atlantic: 1. Dimethylsulfide in sea water and in the atmospheric boundary layer. *Journal of Geophysical Research*, *99*(D11), 22819. <https://doi.org/10.1029/94JD01837>
- Bates, T. S., Quinn, P. K., Coffman, D. J., Johnson, J. E., Miller, T. L., Covert, D. S., et al. (2001). Regional physical and chemical properties of the marine boundary layer aerosol across the Atlantic during Aerosols99: An overview. *Journal of Geophysical Research*, *106*(D18), 20767–20782. <https://doi.org/10.1029/2000JD900578>
- Beale, R., Liss, P. S., & Nightingale, P. D. (2010). First oceanic measurements of ethanol and propanol. *Geophysical Research Letters*. <https://doi.org/10.1029/2010GL045534>
- De Gouw, J. A., Middlebrook, A. M., Warneke, C., Goldan, P. D., Kuster, W. C., Roberts, J. M., et al. (2005). Budget of organic carbon in a polluted atmosphere: Results from the New England Air Quality Study in 2002. *Journal of Geophysical Research - D: Atmospheres*, *110*(16), 1–22. <https://doi.org/10.1029/2004JD005623>
- Gelencsér, A., Siszler, K., & Hlavay, J. (1997). Toluene-benzene concentration ratio as a tool for characterizing the distance from vehicular emission sources. *Environmental Science and Technology*, *31*(10), 2869–2872. <https://doi.org/10.1021/es970004c>

- Gratien, A., Johnson, S. N., Ezell, M. J., Dawson, M. L., Bennett, R., & Finlayson-Pitts, B. J. (2011). Surprising formation of p-cymene in the oxidation of  $\alpha$ -pinene in air by the atmospheric oxidants OH, O<sub>3</sub>, and NO<sub>3</sub>. *Environmental Science and Technology*, 45(7), 2755–2760. <https://doi.org/10.1021/es103632b>
- Hazrati, S., Rostami, R., Fazlzadeh, M., & Pourfarzi, F. (2016). Benzene, toluene, ethylbenzene and xylene concentrations in atmospheric ambient air of gasoline and CNG refueling stations. *Air Quality, Atmosphere and Health*, 9(4), 403–409. <https://doi.org/10.1007/s11869-015-0349-0>
- Hodshire, A. L., Campuzano-Jost, P., Kodros, J. K., Croft, B., Nault, B. A., Schroder, J. C., et al. (2019). The potential role of methanesulfonic acid (MSA) in aerosol formation and growth and the associated radiative forcings. *Atmospheric Chemistry and Physics*, 19(5), 3137–3160. <https://doi.org/10.5194/acp-19-3137-2019>
- Hughey, C. A., Hendrickson, C. L., Rodgers, R. P., Marshall, A. G., & Qian, K. (2001). Kendrick mass defect spectrum: A compact visual analysis for ultrahigh-resolution broadband mass spectra. *Analytical Chemistry*, 73(19), 4676–4681. <https://doi.org/10.1021/ac010560w>
- Jaars, K., Vestenius, M., vanZyl, P. G., Beukes, J. P., Hellén, H., Vakkari, V., et al. (2018). Receptor modelling and risk assessment of volatile organic compounds measured at a regional background site in South Africa. *Atmospheric Environment*, 172, 133–148. <https://doi.org/10.1016/j.atmosenv.2017.10.047>
- Jenkin, M. E., Saunders, S. M., & Pilling, M. J. (1997). The tropospheric degradation of volatile organic compounds: A protocol for mechanism development. *Atmospheric Environment*, 31(1), 81–104. [https://doi.org/10.1016/S1352-2310\(96\)00105-7](https://doi.org/10.1016/S1352-2310(96)00105-7)
- Kristensson, A., Johansson, C., Westerholm, R., Swietlicki, E., Gidhagen, L., Wideqvist, U., & Vesely, V. (2004). Real-world traffic emission factors of gases and particles measured in a road tunnel in Stockholm, Sweden. *Atmospheric Environment*, 38(5), 657–673. <https://doi.org/10.1016/j.atmosenv.2003.10.030>
- Miller, L., Xu, X., Wheeler, A., Atari, D. O., Grgicak-Mannion, A., & Luginaah, I. (2011). Spatial variability and application of ratios between BTEX in two Canadian Cities. *The Scientific World Journal*, 11, 2536–2549. <https://doi.org/10.1100/2011/167973>
- Misztal, P. K., Hewitt, C. N., Wildt, J., Blande, J. D., Eller, A. S. D., Fares, S., et al. (2015). Atmospheric benzenoid emissions from plants rival those from fossil fuels. *Scientific Reports*, 5(June), 1–10. <https://doi.org/10.1038/srep12064>
- Murphy, J. G., Oram, D. E., & Reeves, C. E. (2010). Measurements of volatile organic compounds over West Africa. *Atmospheric Chemistry and Physics*, 10(12), 5281–5294. <https://doi.org/10.5194/acp-10-5281-2010>
- Otter, L., Guenther, A., Wiedinmyer, C., Fleming, G., Harley, P., & Greenberg, J. (2003). Spatial and temporal variations in biogenic volatile organic compound emissions for Africa south of the equator. *Journal of Geophysical Research*, 108(13), 1–12. <https://doi.org/10.1029/2002jd002609>
- Paatero, P. (1997). Least squares formulation of robust non-negative factor analysis. *Chemometrics and Intelligent Laboratory Systems*, 37(1), 23–35. [https://doi.org/10.1016/S0169-7439\(96\)00044-5](https://doi.org/10.1016/S0169-7439(96)00044-5)
- Paatero, P., & Tapper, U. (1994). Positive matrix factorization: A non-negative factor model with optimal utilization of error estimates of data values. *Environmetrics*, 5(2), 111–126. <https://doi.org/10.1002/env.3170050203>
- Saunders, S. M., Jenkin, M. E., Derwent, R. G., & Pilling, M. J. (2003). Protocol for the development of the Master Chemical Mechanism, MCM v3 (Part A): Tropospheric degradation of non-aromatic volatile organic compounds. *Atmospheric Chemistry and Physics*, 3(1), 161–180. <https://doi.org/10.5194/acp-3-161-2003>
- Seizirtger, D. E., Marshall, W. F., Cox, F. W., & Boyd, M. W. (1986). Vehicle evaporative and exhaust emissions as influenced by benzene content of gasoline. *SAE Technical Papers*, 95, 124–151. <https://doi.org/10.4271/860531>
- Skorokhod, A. I., Berezina, E. V., Moiseenko, K. B., Elansky, N. F., & Belikov, I. B. (2017). Benzene and toluene in the surface air of northern Eurasia from TROIICA-12 campaign along the Trans-Siberian Railway. *Atmospheric Chemistry and Physics*, 17(8), 5501–5514. <https://doi.org/10.5194/acp-17-5501-2017>
- Stone, D., Whalley, L. K., & Heard, D. E. (2012). Tropospheric OH and HO<sub>2</sub> radicals: Field measurements and model comparisons. *Chemical Society Reviews*, 41(19), 6348–6404. <https://doi.org/10.1039/c2cs35140d>
- Tsai, W. Y., Chan, L. Y., Blake, D. R., & Chu, K. W. (2006). Vehicular fuel composition and atmospheric emissions in South China: Hong Kong, Macau, Guangzhou, and Zhuhai. *Atmospheric Chemistry and Physics*, 6(11), 3281–3288. <https://doi.org/10.5194/acp-6-3281-2006>
- Van Pinxteren, M., Wadinga Fomba, K., Triesch, N., Stolle, C., Wurl, O., Bahlmann, E., et al. (2020). Marine organic matter in the remote environment of the Cape Verde islands—an introduction and overview to the MarParCloud campaign. *Atmospheric Chemistry and Physics*, 20(11), 6921–6951. <https://doi.org/10.5194/acp-20-6921-2020>
- Warneke, C., McKeen, S. A., deGouw, J. A., Goldan, P. D., Kuster, W. C., Holloway, J. S., et al. (2007). Determination of urban volatile organic compound emission ratios and comparison with an emissions database. *Journal of Geophysical Research*, 112(10). <https://doi.org/10.1029/2006JD007930>
- Yang, M., Beale, R., Liss, P., Johnson, M., Blomquist, B., & Nightingale, P. (2014). Air-sea fluxes of oxygenated volatile organic compounds across the Atlantic Ocean. *Atmospheric Chemistry and Physics*, 14(14), 7499–7517. <https://doi.org/10.5194/acp-14-7499-2014>